Journal of Geophysical Research - Oceans

Supporting Information for

Airborne remote sensing of wave propagation in the marginal ice zone.

Peter Sutherland[1], John Brozena[2], W. Erick Rogers[3], Martin Doble[4], Peter Wadhams[5]

[1]Laboratoire d'Océanographie Physique et Spatiale (LOPS), IFREMER, Plouzané, France
[2]Naval Research Laboratory, Marine Geosciences Division, Washington DC, USA
[3]Naval Research Laboratory, Stennis Space Center, MS, USA
[4]Polar Scientific, Ltd, UK 8
[5]Cambridge University, Cambridge, UK

Contents of this file

Comparisons between wave model results and buoy observations during Flight 4

In the main text, we describe comparisons between the lidar observations and the wave model WAVEWATCH III® ("WW3", Tolman (1991), WW3DG (2016)). In this supplemental document, we described comparisons between the wave model results and drifting buoy observations. These results are presented in a series of figures starting on page S4. The model simulation is described in Rogers et al. (2018) (referred to as "R18" herein). The "IC4M6H" parametrization for dissipation of wave energy by sea ice is used, e.g. as presented in Figure 120 of R18. The buoy notation follows that of R18, e.g. "S09" is SWIFT buoy 9 and "D09" is UK buoy 9. SWIFT buoys (Thomson 2012) are owned and operated by U. Washington Applied Physics Laboratory. Each figure page corresponds to a different buoy. There are three panels on each plot: significant wave height H_{m0}, dominant wave period $T_{m,-1,0}$, and fourth moment of the 1-d spectrum, m_4. Mathematical definitions of the three parameters are given in R18, Section 6.3.2. The parameter m_4 is proportional to mean square slope, and since it is a fourth moment, it is highly responsive to the suppression of high frequency wave energy, e.g. by sea ice. All parameters are computed from consistent integration of 1-d spectra: upper and lower bounds of the integration are the same for both model and buoy. Mean geographic position during Flight 4 is shown at the top of each page. The vertical blue lines indicate the start and end of Flight 4. The buoy deployments correspond to Wave Array 6 (WA6) described in Section 2.2.6 of R18. WA6 was a longer duration than the lidar measurements of Flight 4. The figures here do not include the entirety of WA6, to enhance visibility of the time period of Flight 4 (within the vertical blue lines). All points in the plots represent co-locations in time and space via trilinear interpolation.

In the main text, lidar data for Flight 4 are broken into three groups: 1) farther off-ice, 2) intermediate (in open water close to ice or in ice of low concentration) and 3) in substantial ice. In terms of the drifting buoys, we see a similar separation:

1) S15
2) S14, S13, D02, S11
3) D09, D07, D06, D03, S12, S09

These are referred to herein as group 1, group 2, and group 3. The grouping is according to the suppression of m_4 by ice cover, so group 3 has larger suppression than group 2, which has larger suppression than group 1. In other words, we are using observed m_4 as an indicator for ice cover, and the grouping is according to that ice cover. The geographic position of the buoys, shown at the top of each figure, supports this grouping, with the argument that buoys toward the southwest are more "off-ice" and buoys to the northeast are more "in ice". The only exception is buoy D02, which has a spectrum that suggests light ice cover (group 2) but is relatively far to the east, suggesting that it might belong in group 3. However, we believe that m_4 is a better indicator for ice than geographic position, since ice cover is highly irregular and regions of locally sparse ice cover or "embayments" in the ice field can readily occur, especially near the ice edge.

We make the following observations from the plots:

- In *all* groups, low frequency wave energy is overpredicted. This is consistent with the model vs. lidar comparison in the main text, where we offer two possible explanations: "the model is either overpredicting the generation of wave energy strongly oblique to the wind direction, or is underpredicting the ice along the ice edge to the southeast, that being the up-wave direction of this longer-wave component." The "strongly oblique" direction of these longer waves is discussed further below.
- In group 1 (open water to the southwest), high frequency wave energy is well predicted by the model. This is consistent with the model vs. lidar comparison in the main text.
- In group 2 (intermediate positions), high frequency wave energy is underpredicted. This is consistent with the model vs. lidar comparison in the main text, where we state that it is most likely caused by a local overestimate of ice concentration in the model forcing. In most cases, the overprediction of low frequency wave energy and underprediction of high frequency wave energy results in a fortuitous cancellation of errors in the waveheight comparison. This is why, in the main text, we speculate that the same thing is responsible for the good prediction of wave height relative to the lidar measurements.
- In group 3 (further in the ice), in the main text reports that the model overestimates waveheight by 120%. Such large overprediction is apparent at three (possibly four) of the six buoys in this group.
- In group 3 (further in the ice), the suppression of mean square slope by the sea ice is well predicted. At first, this may seem to be contradicting the finding in the main text, which is that high frequency energy is underpredicted in the model. However, the discrepancy is easily explained. In the text, the spectra are plotted on log scale. While the spectral tails appear dissimilar (lidar vs. model) in these plots, both indicate suppression by the sea ice (weak in the case of lidar, and strong in the case of model). Here, m_4 is plotted on linear scale, so the differences do not appear as large, but both buoy and model indicate very strong suppression m_4 by the sea ice.
- Though the model validation for Flight 4 is largely negative (meaning that the model has low skill near the ice edge), this is one positive outcome: the extreme decrease in

m_4 —near 4× 10^{-4} m^2/s^4 in group 1, dropping to a tiny fraction of that in group 3 — is captured extremely well by the model. This tells us that groups 1 and 3 are far enough from the ice edge that the errors in ice edge position do not have a large effect on prediction of mean square slope, which is dominated by the local ice concentration. Group 2 is "too close" to the ice edge, so ice concentration forcing is less accurate at these positions, which causes inaccurate prediction of m_4 in group 2.

Next, we discuss the **"strongly oblique" direction of the low frequency wave component**. This is from the south-southeast (SSE), approximately from 160° (observed at the ship), and the local wind direction is from east-southeast (ESE), approximately from 100° (also observed at the ship). Thus "strongly oblique" refers to a 60° separation. The reader is referred to a comparison of measurements of wind and wave direction in Figure 19 of R18. In Figure 18 of R18, the model mean wave direction is from the southeast, roughly consistent with these ship measurements. Also, the model mean direction is toward NNW further from the ice and is toward the NW closer to the ice edge. This apparent steering is consistent with the lidar observations, where the locations further in the ice are more strongly influenced by the low frequency component from the SSE. It is important to notice that though the model direction is "toward the northwest" as a result of this swell energy from the SSE, the model wind forcing does *not* include a noticeable southerly component in these southern regions of the grid. This is the reason for our assertion that the low frequency "swell" wave energy was generated by the oblique easterly winds: the same wind system that generates the high frequency energy from the east, observed in the lidar.

In closing: we have found here that the model validation using buoy data gives strikingly similar conclusions to the model validation using lidar data. In fact, the only significant discrepancy is likely caused by dissimilar method of comparison (mean square slope on linear scale vs. high frequency energy spectral density on log scale). This agreement improves our confidence in the utility of both methods.

References

Rogers, W.E., P. Posey, L. Li, R.A. Allard (2018). Forecasting and hindcasting waves in and near the marginal ice zone: Wave modeling and the ONR "Sea State" field experiment, NRL Report NRL/MR/7320--18-9786, 179 pp. [available from www7320.nrlssc.navy.mil/pubs.php].

Thomson, J. (2012). Wave breaking dissipation observed with SWIFT drifters, *J. Atmos. Ocean. Tech., 29*, 1866–1882, doi:10.1175/JTECH-D-12-00018.1.

Tolman, H. L. (1991), A Third-generation model for wind-waves on slowly varying, unsteady, and inhomogeneous depths and currents, *J. Phys. Oceanogr.* **21**(6*),* 782-797.

The WAVEWATCH III® Development Group (WW3DG) (2016), User manual and system documentation of WAVEWATCH III® version 5.16. Tech. Note 329, NOAA/NWS/NCEP/MMAB, College Park, MD, USA, 326 pp. + Appendices.

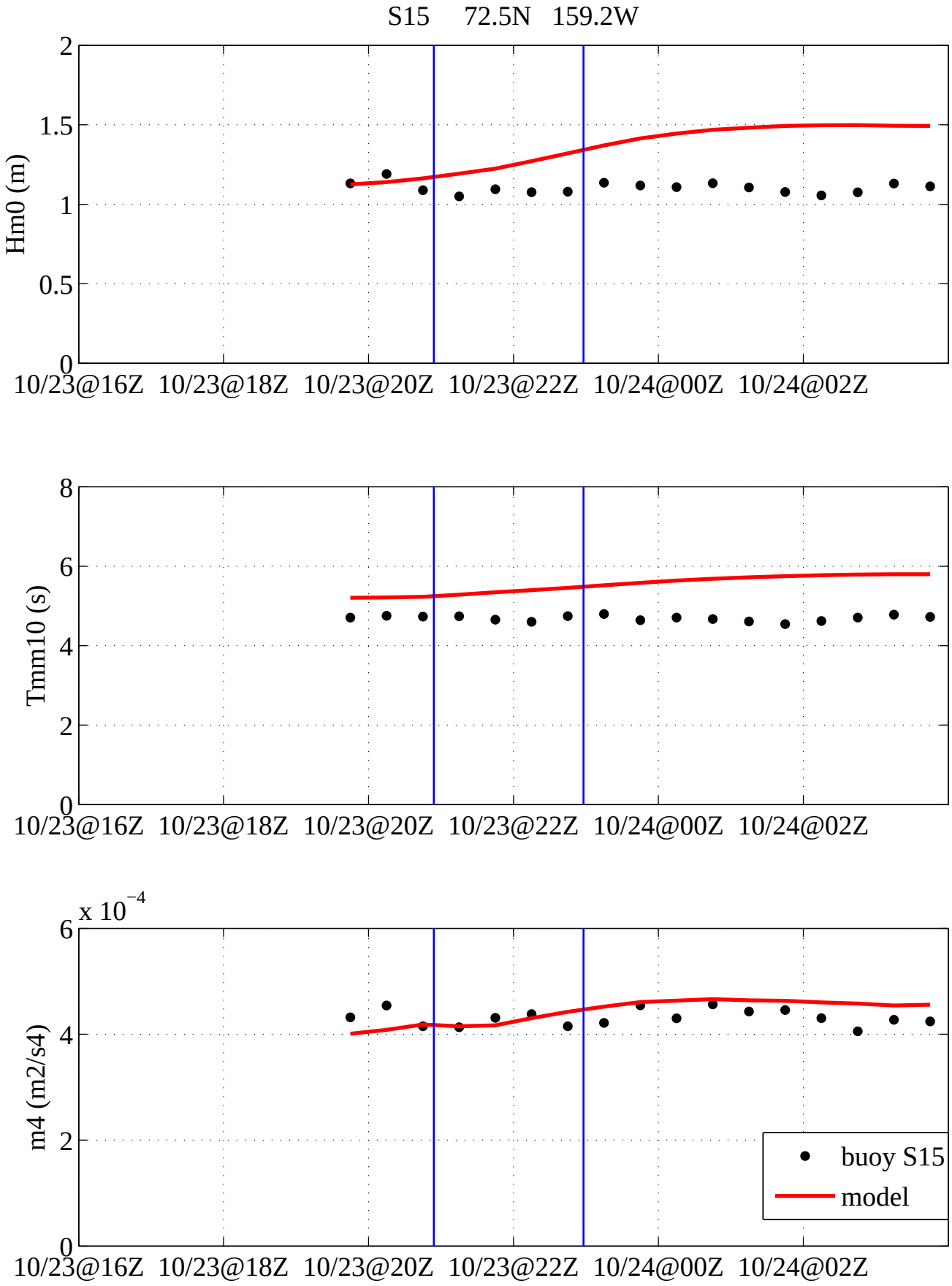
S15 72.5N 159.2W
Hm0 (m)
2
1.5
1
0.5
0
10/23@16Z
10/23@18Z
10/23@20Z
10/23@22Z
10/24@00Z
10/24@02Z
Tmm10 (s)
8
6
4
2
0
10/23@16Z
10/23@18Z
10/23@20Z
10/23@22Z
10/24@00Z
10/24@02Z
x 10^-4
m4 (m2/s4)
6
4
2
0
buoy S15
model
10/23@16Z
10/23@18Z
10/23@20Z
10/23@22Z
10/24@00Z
10/24@02Z

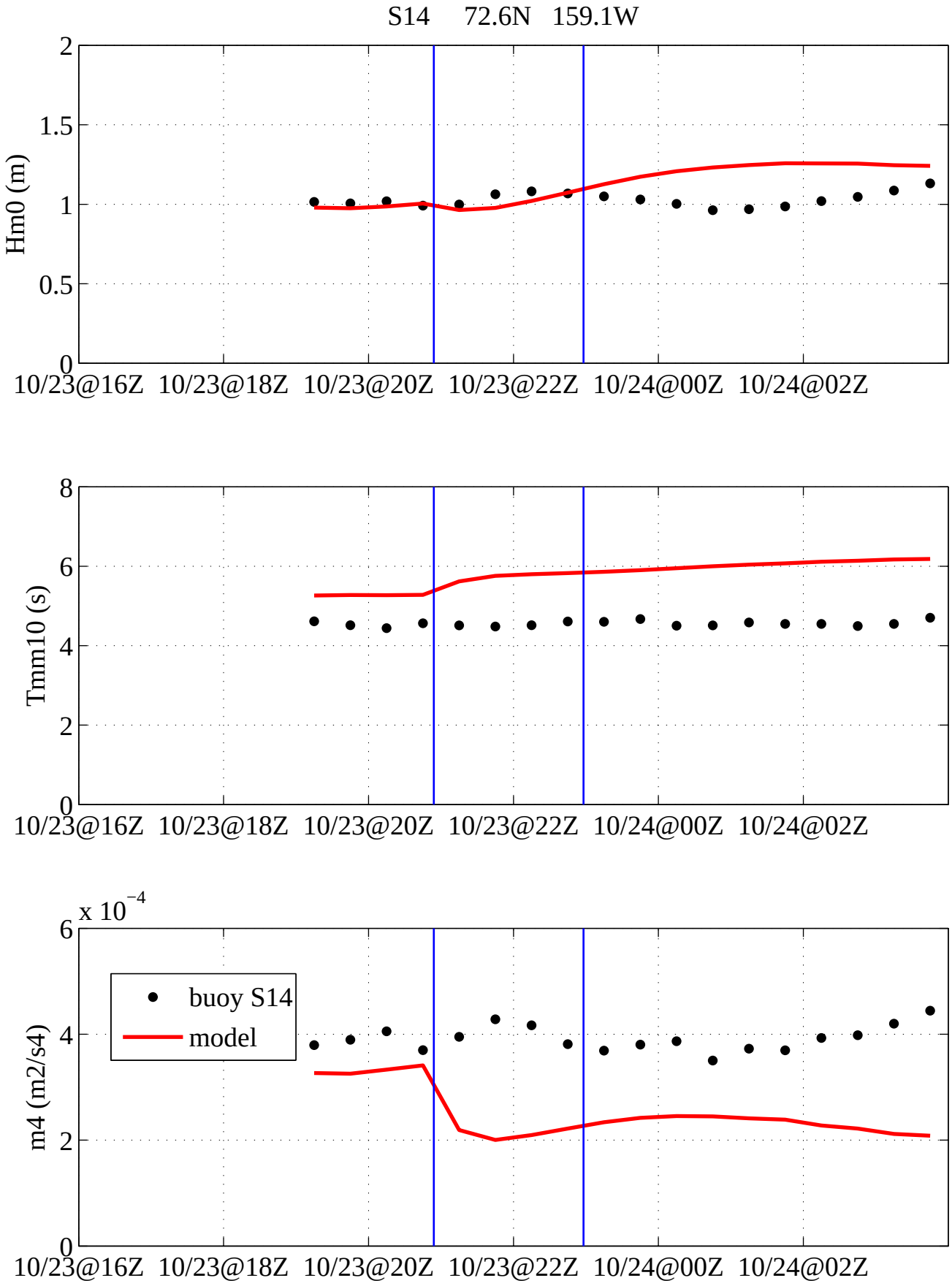
S14 72.6N 159.1W
Hm0 (m)
2
1.5
1
0.5
0
10/23@16Z
10/23@18Z
10/23@20Z
10/23@22Z
10/24@00Z
10/24@02Z
Tmm10 (s)
8
6
4
2
0
10/23@16Z
10/23@18Z
10/23@20Z
10/23@22Z
10/24@00Z
10/24@02Z
x 10^-4
m4 (m2/s4)
6
4
2
0
buoy S14
model
10/23@16Z
10/23@18Z
10/23@20Z
10/23@22Z
10/24@00Z
10/24@02Z

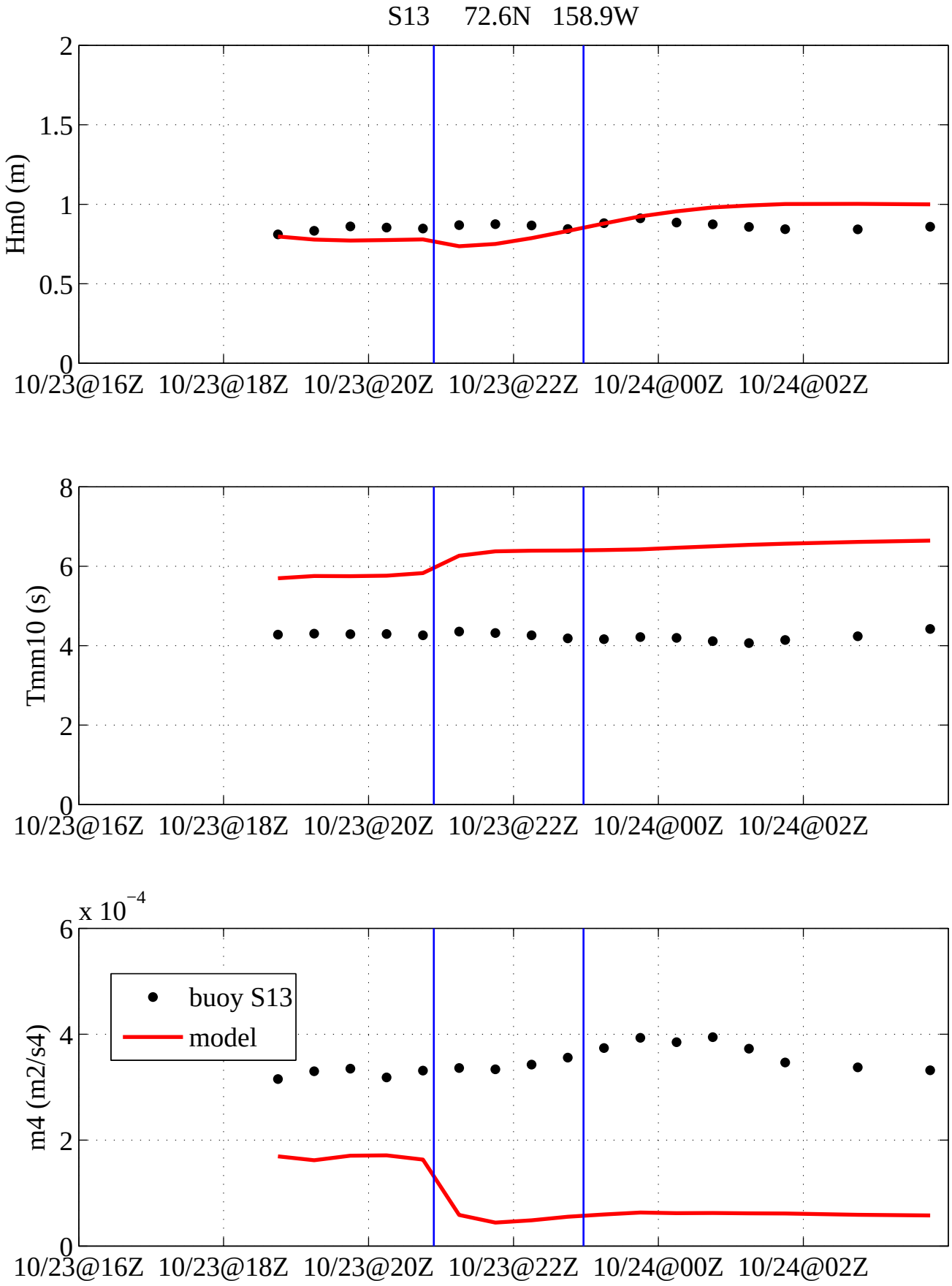
S13 72.6N 158.9W
Hm0 (m)
2
1.5
1
0.5
0
10/23@16Z
10/23@18Z
10/23@20Z
10/23@22Z
10/24@00Z
10/24@02Z
Tmm10 (s)
8
6
4
2
0
10/23@16Z
10/23@18Z
10/23@20Z
10/23@22Z
10/24@00Z
10/24@02Z
x 10^-4
m4 (m2/s4)
6
4
2
0
buoy S13
model
10/23@16Z
10/23@18Z
10/23@20Z
10/23@22Z
10/24@00Z
10/24@02Z

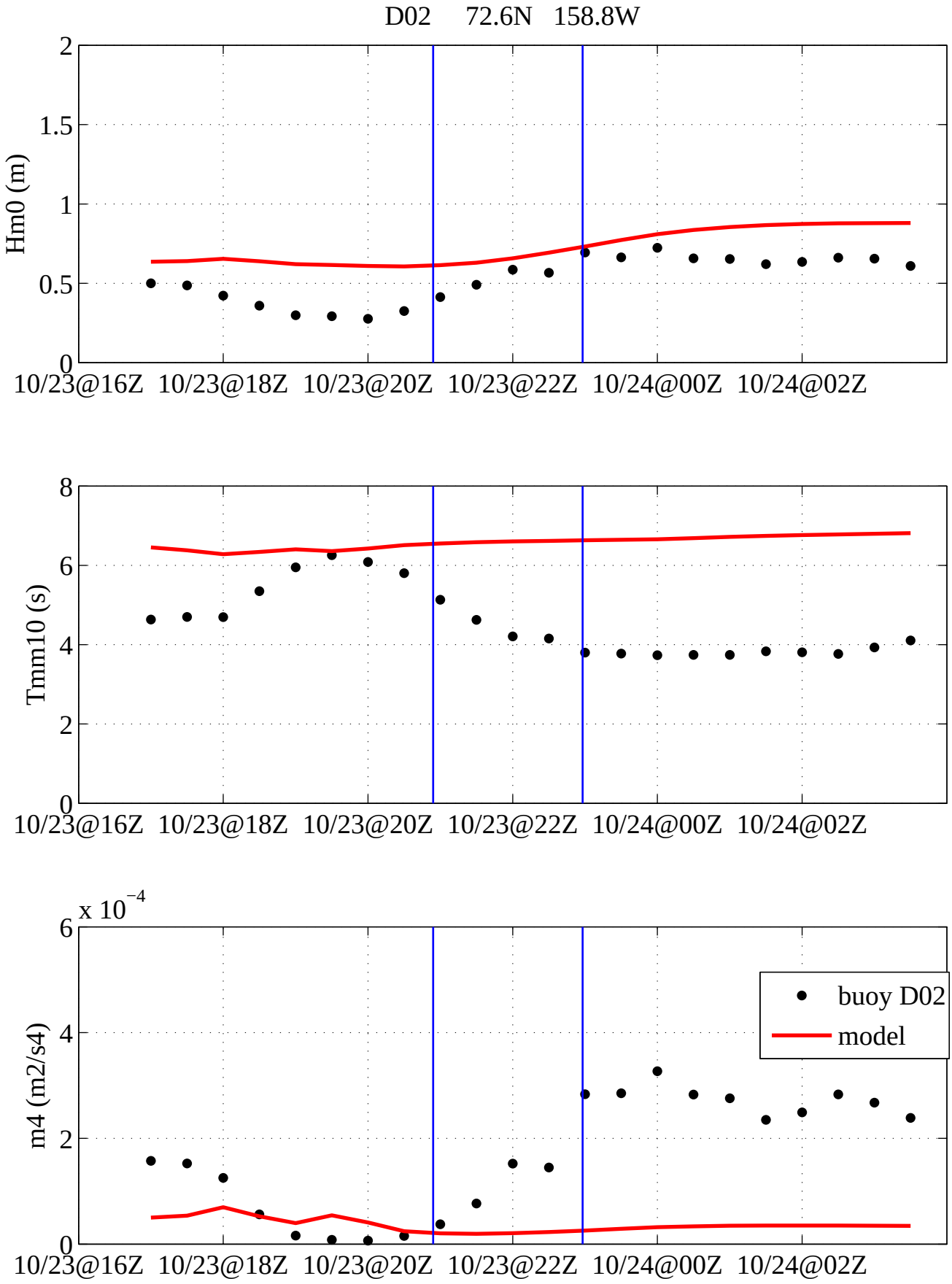
D02 72.6N 158.8W
Hm0 (m)
2
1.5
1
0.5
0
10/23@16Z
10/23@18Z
10/23@20Z
10/23@22Z
10/24@00Z
10/24@02Z
Tmm10 (s)
8
6
4
2
0
10/23@16Z
10/23@18Z
10/23@20Z
10/23@22Z
10/24@00Z
10/24@02Z
x 10^-4
m4 (m2/s4)
6
4
2
0
buoy D02
model
10/23@16Z
10/23@18Z
10/23@20Z
10/23@22Z
10/24@00Z
10/24@02Z

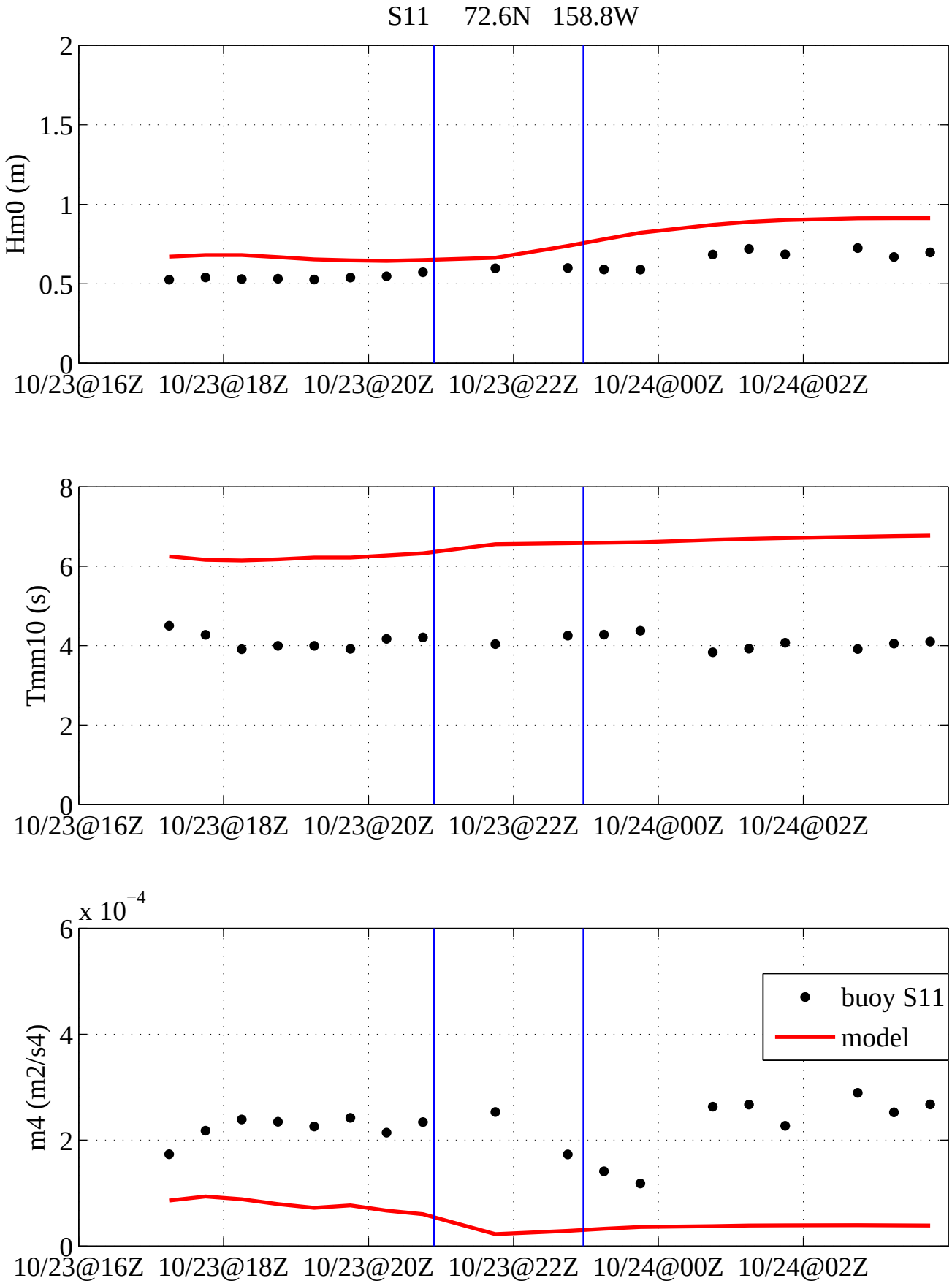
S11 72.6N 158.8W
Hm0 (m)
2
1.5
1
0.5
0
10/23@16Z
10/23@18Z
10/23@20Z
10/23@22Z
10/24@00Z
10/24@02Z
Tmm10 (s)
8
6
4
2
0
10/23@16Z
10/23@18Z
10/23@20Z
10/23@22Z
10/24@00Z
10/24@02Z
x 10^-4
m4 (m2/s4)
6
4
2
0
buoy S11
model
10/23@16Z
10/23@18Z
10/23@20Z
10/23@22Z
10/24@00Z
10/24@02Z

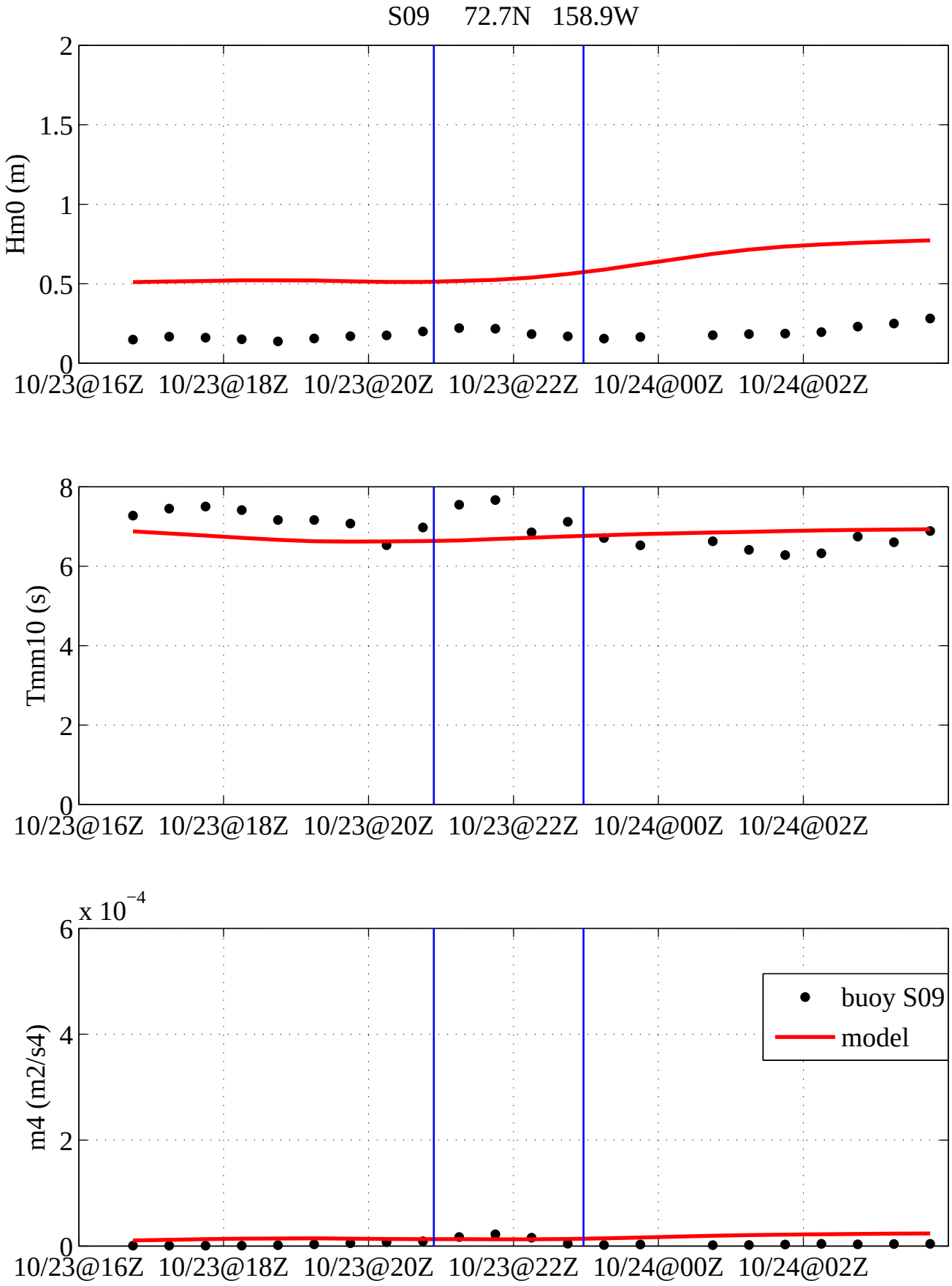
S09 72.7N 158.9W
Hm0 (m)
2
1.5
1
0.5
0
10/23@16Z
10/23@18Z
10/23@20Z
10/23@22Z
10/24@00Z
10/24@02Z
Tmm10 (s)
8
6
4
2
0
10/23@16Z
10/23@18Z
10/23@20Z
10/23@22Z
10/24@00Z
10/24@02Z
x 10^-4
m4 (m2/s4)
6
4
2
0
buoy S09
model
10/23@16Z
10/23@18Z
10/23@20Z
10/23@22Z
10/24@00Z
10/24@02Z

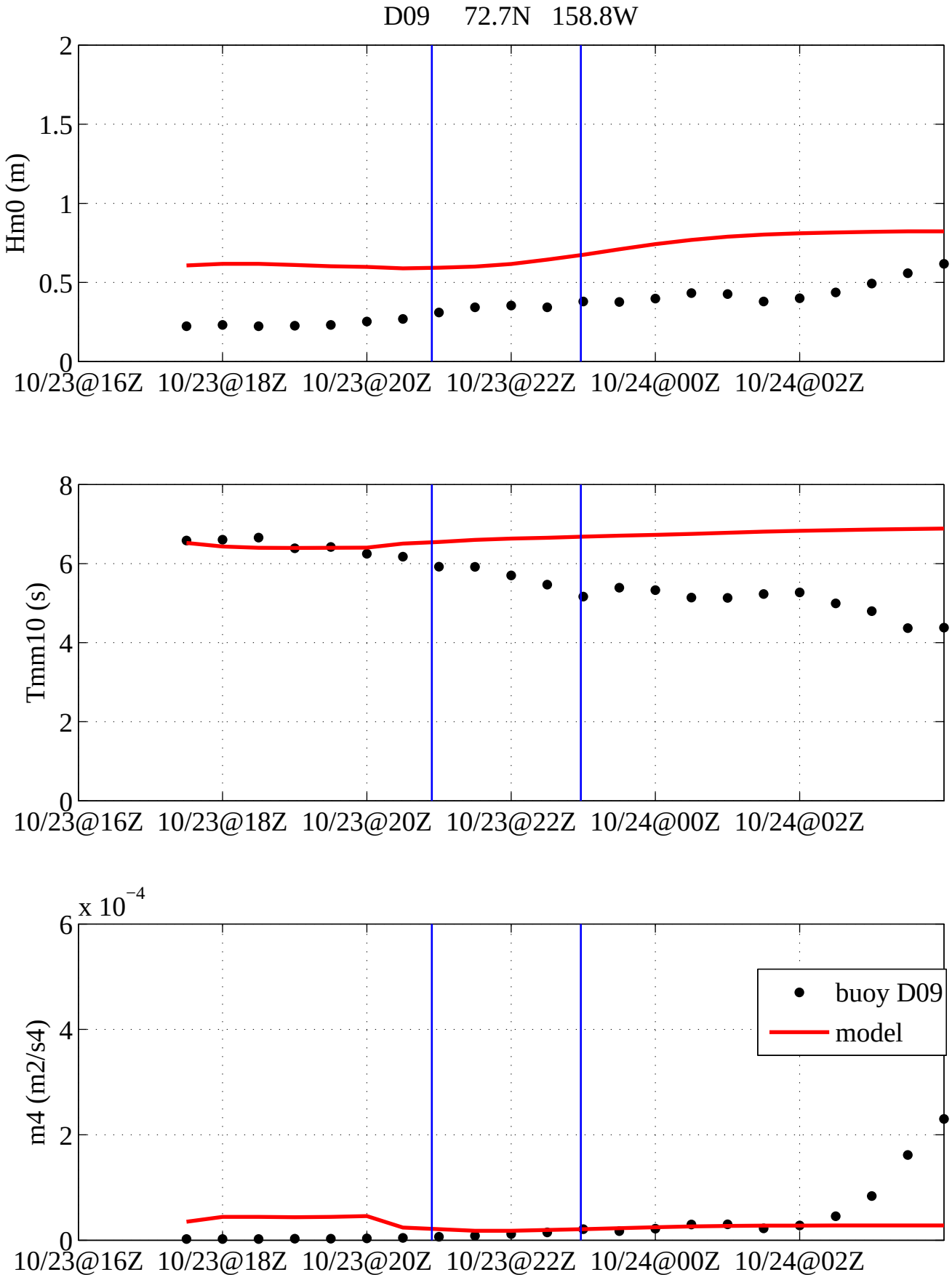
D09 72.7N 158.8W
Hm0 (m)
2
1.5
1
0.5
0
10/23@16Z
10/23@18Z
10/23@20Z
10/23@22Z
10/24@00Z
10/24@02Z
Tmm10 (s)
8
6
4
2
0
10/23@16Z
10/23@18Z
10/23@20Z
10/23@22Z
10/24@00Z
10/24@02Z
x 10^-4
m4 (m2/s4)
6
4
2
0
buoy D09
model
10/23@16Z
10/23@18Z
10/23@20Z
10/23@22Z
10/24@00Z
10/24@02Z

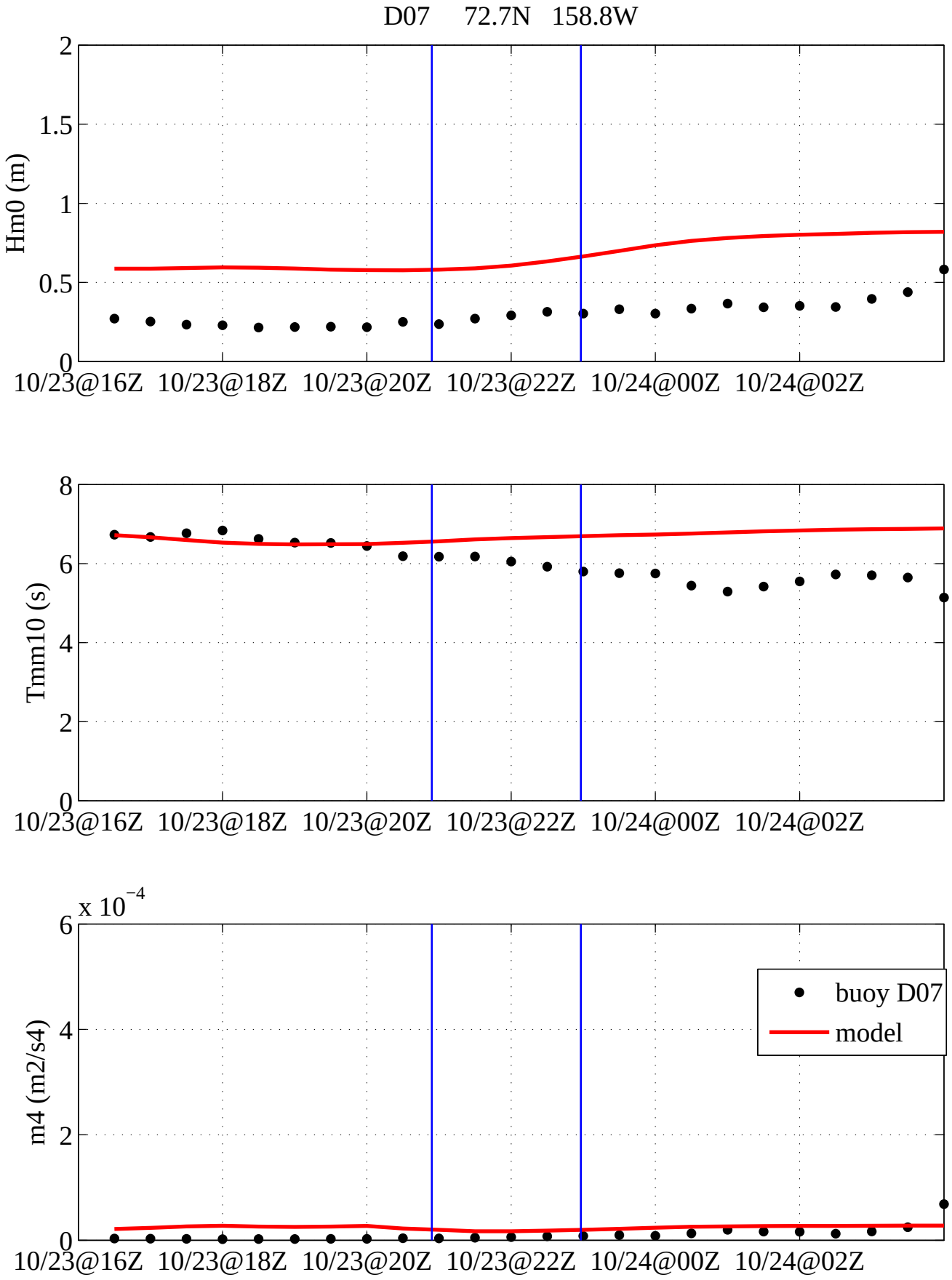
D07 72.7N 158.8W
Hm0 (m)
2
1.5
1
0.5
0
10/23@16Z 10/23@18Z 10/23@20Z 10/23@22Z 10/24@00Z 10/24@02Z
Tmm10 (s)
8
6
4
2
0
10/23@16Z 10/23@18Z 10/23@20Z 10/23@22Z 10/24@00Z 10/24@02Z
x 10^-4
m4 (m2/s4)
6
4
2
0
buoy D07
model
10/23@16Z 10/23@18Z 10/23@20Z 10/23@22Z 10/24@00Z 10/24@02Z

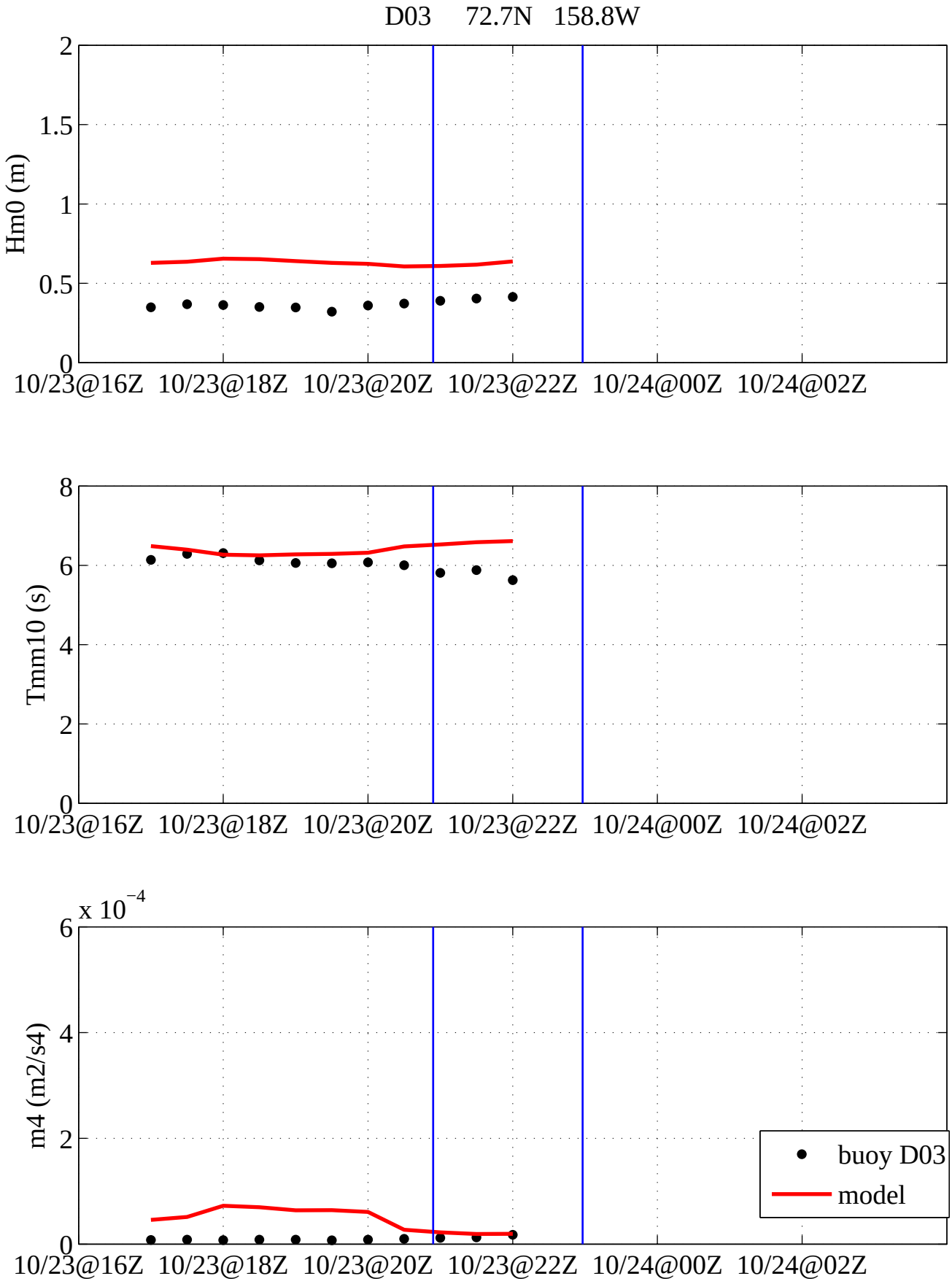
D03 72.7N 158.8W
Hm0 (m)
2
1.5
1
0.5
0
10/23@16Z
10/23@18Z
10/23@20Z
10/23@22Z
10/24@00Z
10/24@02Z
Tmm10 (s)
8
6
4
2
0
x 10^-4
m4 (m2/s4)
buoy D03
model

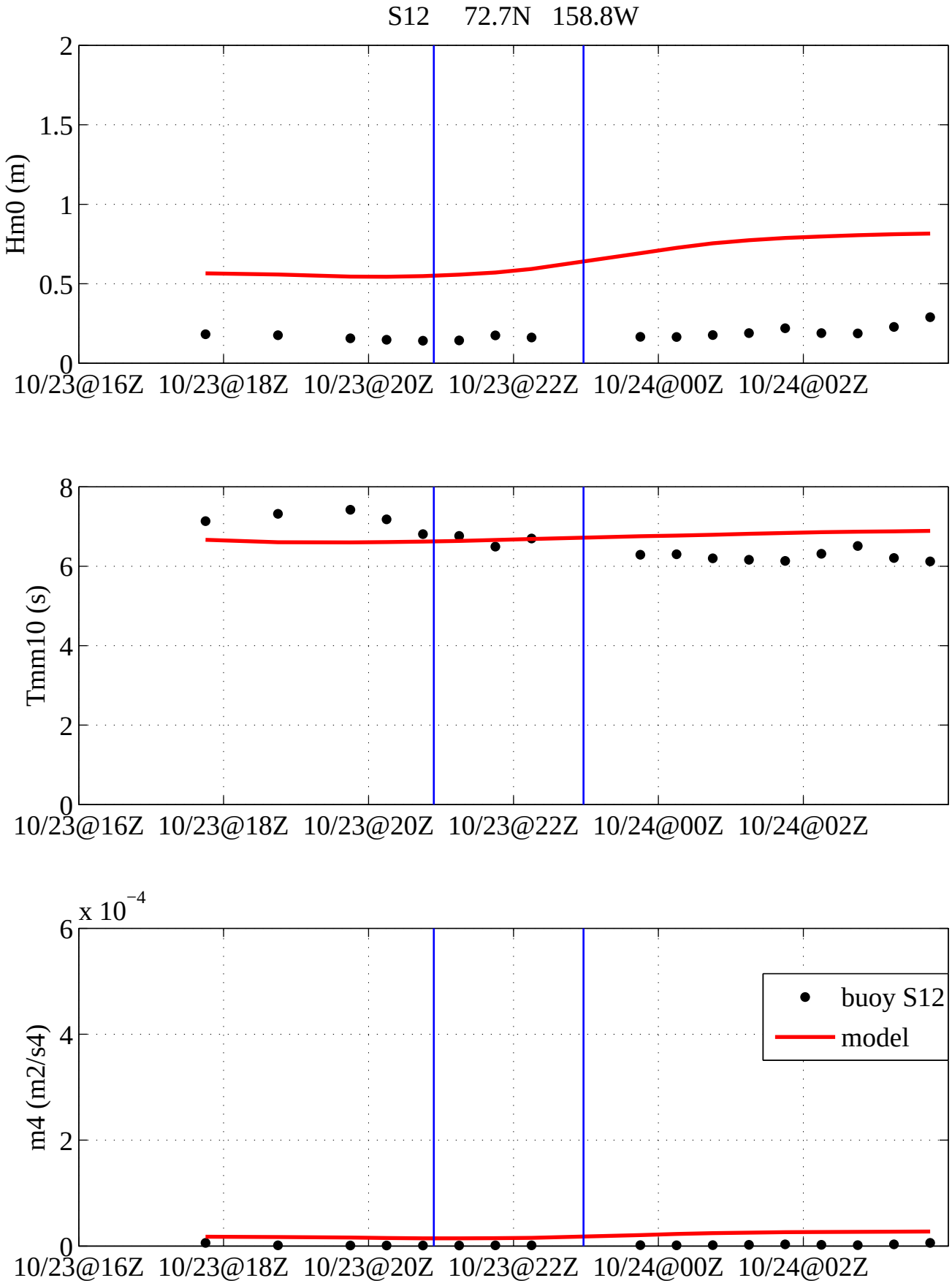
S12 72.7N 158.8W
Hm0 (m)
2
1.5
1
0.5
0
10/23@16Z
10/23@18Z
10/23@20Z
10/23@22Z
10/24@00Z
10/24@02Z
Tmm10 (s)
8
6
4
2
0
10/23@16Z
10/23@18Z
10/23@20Z
10/23@22Z
10/24@00Z
10/24@02Z
x 10^-4
m4 (m2/s4)
6
4
2
0
buoy S12
model
10/23@16Z
10/23@18Z
10/23@20Z
10/23@22Z
10/24@00Z
10/24@02Z

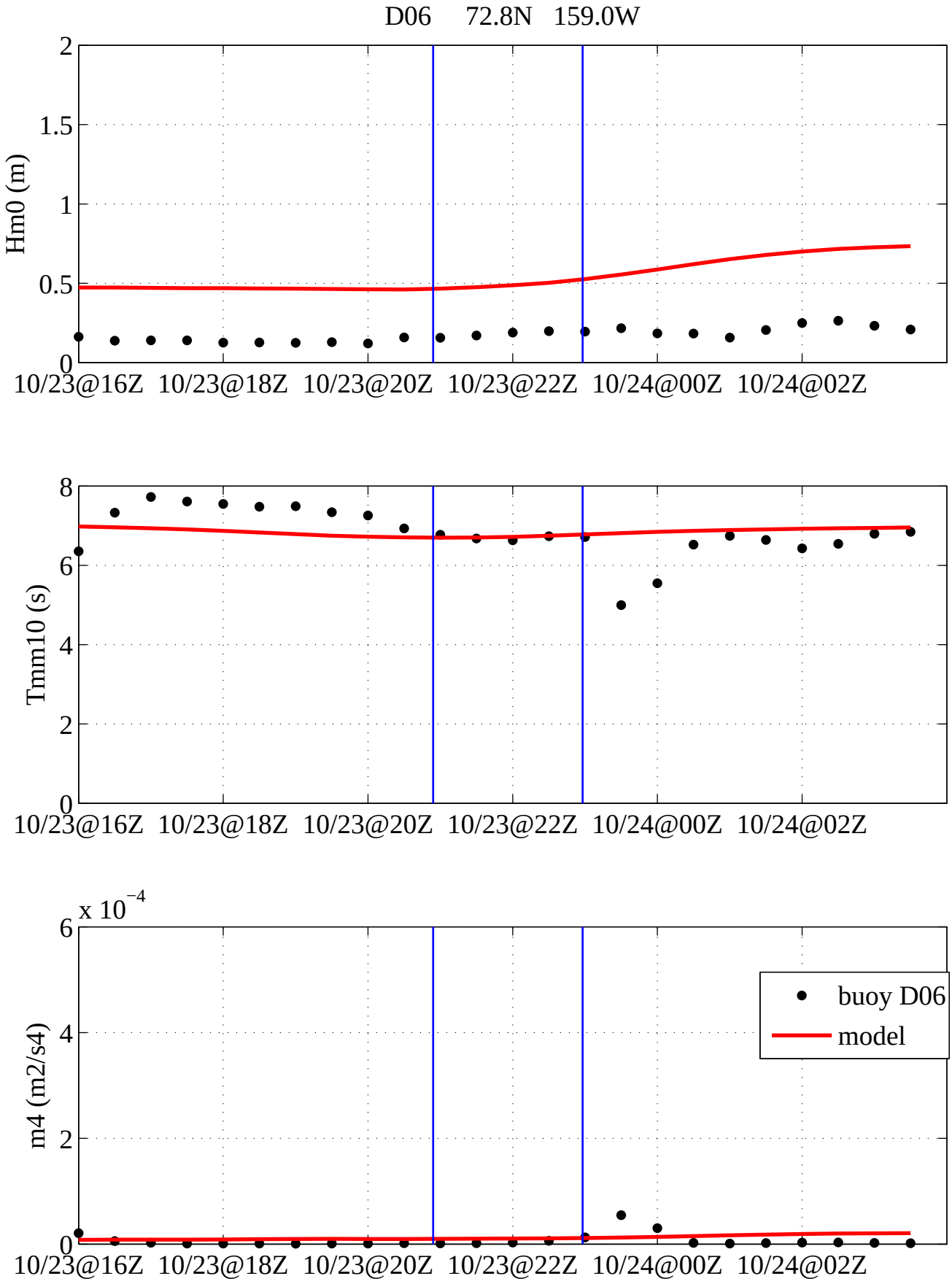
D06 72.8N 159.0W
Hm0 (m)
2
1.5
1
0.5
0
10/23@16Z 10/23@18Z 10/23@20Z 10/23@22Z 10/24@00Z 10/24@02Z
Tmm10 (s)
8
6
4
2
0
10/23@16Z 10/23@18Z 10/23@20Z 10/23@22Z 10/24@00Z 10/24@02Z
x 10^-4
m4 (m2/s4)
6
4
2
0
buoy D06
model
10/23@16Z 10/23@18Z 10/23@20Z 10/23@22Z 10/24@00Z 10/24@02Z